INSTABILITIES IN CURRENT-MODE CONTROLLED SWITCHING VOLTAGE REGULATORS

Richard Redl Istvan Novak

Technical University of Budapest
Budapest, Hungary

ABSTRACT

A survey of the instabilities of switching voltage regulators with different types of current-mode controllers (including LC^3 or constant-hysteresis; MC^2 or constant-frequency and constant off-time versions) is presented.

Apart from the well-known open-loop oscillation of the constant frequency regulator above 50% duty ratio, other instabilities can also arise by increasing the ac loop-gain. At the constant-hysteresis controller the operating frequency changes, at the other types continuously or hysteretically arising subharmonic oscillation appears. These phenomena can be analysed by taking into account the effect of the amplified and fed-back ripple voltage to the operation of the current comparator. Calculations were accomplished in order to establish maximum usable ac gains for the three basic power converter topologies (buck, boost and buck-boost) and for the above mentioned controllers. Experiments were also carried out for several particular power circuit and controller combinations showing close correspondence to theoretical results.

1. INTRODUCTION

Current-mode control is one of the two-loop control methods used at regulated switching power converters. It has been known since 1967 [1] but it was never reported publicly. It was re-invented ten years later [2] and since then it went through a considerable development. Several communications treated different modelling and dynamic analysis aspects of the originnal version (LC^3 or constant hysteresis) or presented and analysed partially modified controller concepts [3]-[11]. An interesting possibility of current-mode control - the use of input voltage/output current feedforward to the input of the current comparator in order to improve the dynamic behavior of the regulator - was also published [12]. However little attention was paid to the question of the maximum usable ac gain of the control loop. Partial results were submitted in [6] and [13] for some of the controller configurations without extra compensation and in [7] for constant-frequency controller with sawtooth compensation. This latter one is a direct combination of the traditional duty-ratio modulation and current-mode control and its characteristics are function of the ratio between the amplitudes of sensed switch current and sawtooth waveform.

Current-mode control of switching power converters has many advantages over PWM control. The peak current of the power switch(es) directly follows the command signal originating from the error amplifier. Thus the inductor is practically removed from the system, resulting in a decrease by one in the number of poles of the characteristics functions. The end result is faster transient response, easier-to-design control loop as well as instantaneous overload protection, possibility to parallel operation of identical power stages without extra current equalization, etc. The benefits are abundantly discussed in most of the papers on current-mode control. However these benefits can be fully exploited only if the gain of the control loop is as high as allowed by the stability requirements of the system. The higher the gain, the smaller is the amplitude of transient response to step load or line changes. The maximum usable ac gain is a function of power circuit topology, type of controlling method and the actual values of the components and steady-state currents/voltages.

The aim of this paper is to give general insight into the mechanisms which produce instability at different power circuit and controller combinations and to introduce simple and easy-to-use analytical methods and expressions for the determination of the maximum usable gain. The essence of the method used throughout the paper is to investigate the effect of the amplified and fed-back output ripple voltage to the operation of the current comparator. The authors strongly believe that

CH1652-7/81/0000-0017 $00.75 © 1981 IEEE

this approach is a useful and easy-to-understand one and despite its relative simplicity it gives results which are accurate enough for everyday applications. It can be extended to compensated operation [5], [7], too.

1.1. Review of current-mode controlling techniques

The common property of all current-mode controlling techniques is the direct command of the peak current of the active switching device(s). The block schematic of the implementation of the simplest and most wide-spread versions in shown in Fig.1.

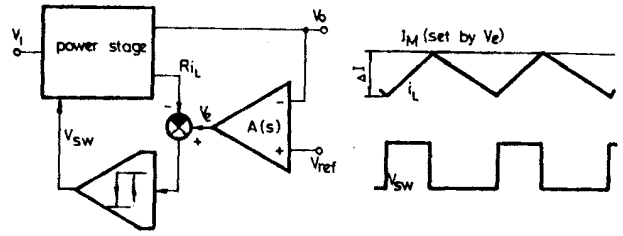

a) constant hysteresis or LC^3 controller

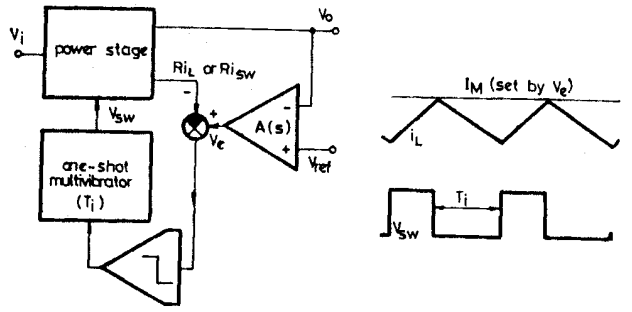

b) constant off-time controller

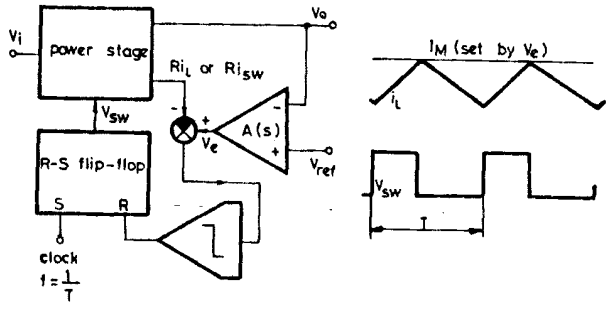

c) constant frequency or MC^2 controller

Fig.1. Basic current-mode controlling techniques

The maximum current of the switch or inductor is set by the output voltage v_e of the error amplifier. The switch is turned off if the voltage on the current sensing element exceeds v_e. The switch can be turned on: (a) after a fixed amount of current decrease in the inductor,
(b) after a fixed time interval or
(c) by a clock signal of fixed frequency.

The error amplifier of the regulating loop can be implemented as shown Fig.2. Using a high dc gain amplifier the frequency response can be approximated as shown in the same figure. This solution provides zero dc error and constant amplification factor above the characteristic pole frequency ω_o. The value of the gain above ω_o determines the transient response of the regulator.

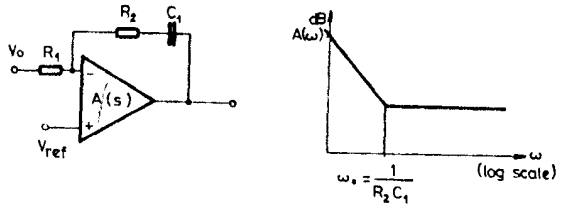

Fig.2 Error amplifier circuit and plot of frequency response

In order to obtain maximum phase margin for the overall feedback control system ω_o must be selected so that the error amplifier together with the rest of the circuit should produce the response of an ideal integrator [12]. Nevertheless this approach does not provide automatically stable operation at high ac loop gain. The reason is, as it will be clarified later, the presence of the amplified output ripple voltage at the input of the current comparator.

For the sake of completeness three additional controlling techniques are introduced in Figs.3 and 4.

Fig.3 shows the block schematic of the slope-compensated controller. As it is long known [14] converters with constant-frequency peak current controllers are unstable, even with open voltage regulating loop, above 50% duty ratio. Deisch [5] proposed a solution to overcome this limitation. The idea is to alter the effective current slopes by adding artificial compensating waveform to the inductor or switch current. Similar technique was used by Pivit and Saxarra [7], but their compensating function was a simple sawtooth waveform.

The constant-on-time controller can be seen in Fig.4a. It differs from the previous versions in one fundamental property. Here, in contrary to the other techniques, the current minimum is commanded directly by the error amplifier. This results in

some difficulties with the voltage regulation at light load. This is the reason why it is not as widely used as the other solutions introduced so far.

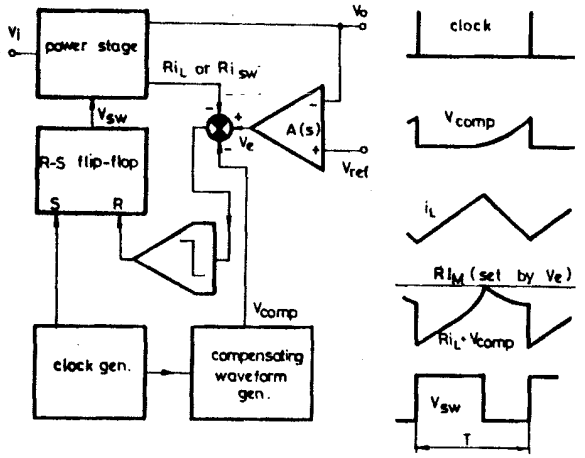

Fig.3 Slope-compensated current-mode controller

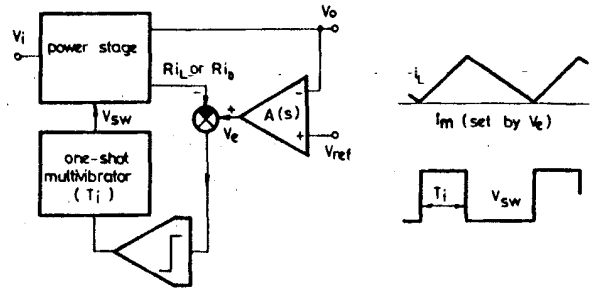

a.) constant on-time controller

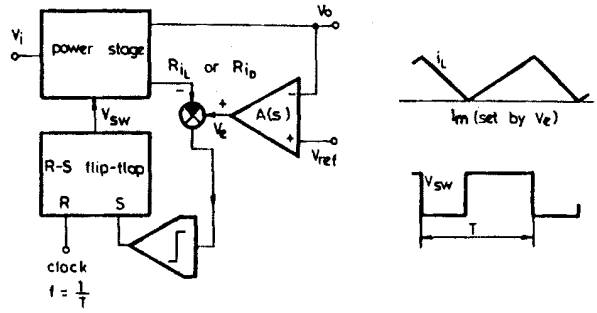

b.) constant - frequency controller

Fig.4 Controllers commanding current minimum

That is the same with the arrangement of Fig.4b, which shows the constant-frequency variation of the current-minimum-controlled converters. It is interesting to note that this controller is open-loop stable only above 50% duty ratio. With compensating technique similar to that of Fig.3, however, it can be used below 50%, too.

2. FREQUENCY SHIFT OF CONVERTERS WITH CONSTANT-HYSTERESIS CONTROLLER

Practical experience shows that switching voltage regulators with constant-hysteresis controllers never display spurious oscillation or other instability of the regulating loop if the usual low-frequency stability criteria of the control system are met. Of course, the excess phase shift of extra input/output filters or of the error amplifier can produce unstable operation but this can be analysed by the help of traditional methods of control theory. However a deeper insight into the operation of the system discovers one particular type of instability, namely: shift of the frequency of free-running oscillation. The fed-back output ripple voltage changes the actual frequency up- or downward, depending on the type of converter. The amount of change is a function of the ac loop gain. Although the frequency shift is not instability in the usual meaning of the word still it is mostly unwanted because it can cause increased dynamic losses or increased ripple current and voltage. If the frequency-versus-gain function is known the ac gain and operating frequency requirements can be maintained by proper design. Also the effect of ageing of components (e.g. change of ESR of the output filter capacitor) can be taken into account.

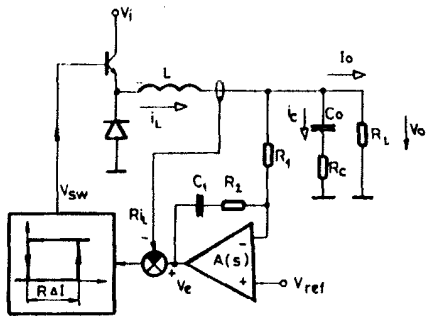

Fig.5 Buck regulator model

As an example the derivation of the frequency-gain relation will be shown for the buck regulator (Fig.5). The relevant waveforms are displayed in Fig.6. The solid line indicates the inductor current. This is one input signal of the current comparator. The other input signal is the error voltage v_e divided by the resistance

R of the current-sensing resistor and shifted in every turn-off interval downward by the current hysteresis ΔI. These sudden jumps represent the hysteretic behavior of the comparator. The waveforms clearly indicate that, due to the ripple component of the error voltage, the effective hysteresis changes and in the particular case of the buck regulator its value, ΔI′ will be less than the pre-set hysteresis ΔI.

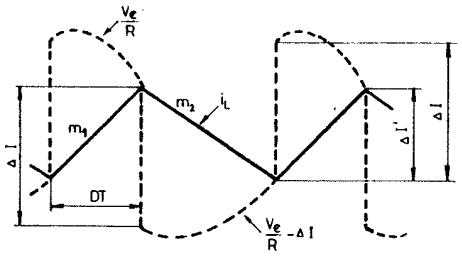

Fig.6 Current comparator waveforms of the buck regulator with constant-hysteresis controller

The following equation can be written for the conducting transistor:

$$\Delta I = \frac{1}{R}\left[v_e(0)-v_e(DT)\right] = m_1 DT \qquad (1)$$

which is the switch-over condition of the current comparator. Here m_1 is the slope of the inductor current during the conduction of the switch, D is the duty ratio, T is the period time. Assuming constant load current and constant ac gain of the error amplifier at and above the operating frequency one can write:

$$\frac{1}{R}\left[v_e(0)-v_e(DT)\right] = g\left[v_o(DT)-v_o(0)\right] \qquad (2)$$

and

$$v_o(DT)-v_o(0)=\left[i_c(DT)-i_c(0)\right]R_c+\frac{1}{C_o}\int_0^{DT} i_c(t)dt \qquad (3)$$

Here

$$i_c(t) = m_1\left(t - \frac{DT}{2}\right) \qquad (4)$$

and

$$g = \frac{R_2}{R\,R_1} \qquad (5)$$

Substituting Eq.(4) into Eq.(3) gives

$$v_o(DT) - v_o(0) = m_1 DTR_c \qquad (6)$$

The effective hysteresis

$$\Delta I' = m_1 DT \qquad (7)$$

can be expressed from Eqs(1), (2) and (6).

$$\Delta I' = \frac{\Delta I}{1+gR_c} \qquad (8)$$

The frequency of operation is inversely proportional to the effective hysteresis. Its value is

$$f = f_o\,(1 + gR_c) \qquad (9)$$

where (neglecting second-order effects) the self-oscillating frequency without ripple feedback is given by the following expression:

$$f_o = \frac{V_o(1-D)}{L\Delta I} \qquad (10)$$

Similar considerations apply to the other converter types. The results are collected in Table 1.

TABLE 1. FREQUENCY OF CONSTANT HYSTERESIS CURRENT-CONTROLLED CONVERTERS WITH AND WITHOUT RIPPLE FEEDBACK

Buck	$f=f_o(1+gR_c)$	$f_o=\frac{V_o(1-D)}{L\Delta I}$
Boost	$f=f_o\frac{1+g\left[\frac{R_c}{2}-\frac{LI_o}{C_oV_o(1-D)}\right]}{1+g\frac{I_oR_c}{\Delta I(1-D)}}$	$f_o=\frac{V_o(1-D)D}{L\Delta I}$
Buck--boost	$f=f_o\frac{1+g\left[\frac{R_c}{2}-\frac{LI_oD}{C_oV_o(1-D)}\right]}{1-g\frac{I_oR_c}{\Delta I(1-D)}}$	$f_o=\frac{-V_o(1-D)}{L\Delta I}$

In the case of the buck regulator the effect of the fed-back ripple is increased frequency. The relative difference is the product of the transconductance of the loop and the equivalent series resistance of the filter capacitor. In the other two cases the actual frequency depends on the output voltage, load current, duty ratio, choke inductance and ESR and capacitance of the filter capacitor. At the usual circuit parameter combinations the frequency generally decreases with increasing loop gain.

The expressions in Table 1 give possibility to forecast the effect of changes in component values to the operating frequency. Because large deviations from the nominal frequency in both directions are unwanted they formulate the real loop gain limit of converters with constant-hysteresis controllers.

3. CONDITIONS OF LOCAL STABILITY OF CONVERTERS WITH CONSTANT-FREQUENCY CONTROLLER

Constant-frequency current-mode controlled converters are subject to spurious oscillation at the first subharmonic of the clock frequency. This fact is not surprising when one realizes that these conver-

ters are prone to instability at the same frequency even with open feedback loop above 50% duty ratio. The open loop transient response shows damped ringing below 50%. The damping factor is a function of the actual duty ratio.

At closed feedback loop subharmonic oscillation also appears above a specific gain value. Depending on the circuit parameters, two different types of this oscillation are possible. At the first type the starting and ceasing gain values are not equal: thus the appearance of the instability is a hysteretic function of the loop gain. This phenomenon will be discussed in detail in the next section of the paper. The other type is characterized by gradually increasing or decreasing magnitude of the oscillation. The starting and ceasing gain values coincide, so there is no hysteresis in the gain at the boundary of instability.

The maximum allowable gain of this continuously arising oscillation was investigated in [13] for the buck and the boost regulator. The method used there was the so-called describing function analysis. This is a well known and useful tool of control theory but, due to its inherent limitations, it is not very accurate. Here an other method will be used which gives better accuracy and can be rather easily applied for the determination of the local stability of current-mode controlled converters.

Essentially this is a perturbation analysis. A system is locally stable if the amplitude of any small perturbation decreases with time or - in the case of sampling type control systems - with the number of subsequent periods. The application of the method is formally very simple. Inject small perturbations in the energy storing elements of the system, i.e. perturb the state variables by infinitesimally small quantities. Calculate the response of the system in the next period and compare it with the excitation. If the magnitude of the response is equal to or larger than the excitation the system is locally unstable.

Mathematically the method is as follows. Let $\underline{u}$ be the vector of infinitesimal perturbations. $\underline{u}$ has as many components as the number of state variables in the system. Let $\underline{v}$ be the response vector. The two vectors are connected by the perturbation matrix of the system:

$$\underline{v} = \underline{\underline{A}}\,\underline{u} \tag{11}$$

There is a special $\underline{u}_i$ vector which produces a response vector $\underline{v}_i$ proportional to $\underline{u}_i$.

$$\underline{v}_i = \lambda\,\underline{u}_i \tag{12}$$

$\underline{u}_i$ is called the eigenvector and λ is called the eigenvalue of the matrix $\underline{\underline{A}}$. If the absolute value of λ is equal to 1 the system is at the verge of local instability.

Hence the condition for stability is:

$$|\lambda| < 1$$

For the eigenvector the following equation applies:

$$\underline{\underline{A}}\,\underline{u}_i = \lambda\,\underline{u}_i \tag{13}$$

This equation has a nontrivial solution if the determinant of the matrix $\underline{\underline{A}}-\lambda\underline{\underline{I}}$ is zero ($\underline{\underline{I}}$ is the unit matrix). That is:

$$|\underline{\underline{A}} - \lambda\underline{\underline{I}}| = 0 \tag{14}$$

Solving Eq.(14) results in the eigenvalues of $\underline{\underline{A}}$.

In our case the most suitable moment for the perturbation is the turn-on instant. Because the perturbation is infinitesimally small the system can be considered linear. Assuming a constant-gain error amplifier there are only two energy-storing elements in the system, so $\underline{\underline{A}}$ is a second-order quadratic matrix. This means that Eq.(14) is a quadratic equation for the eigenvalues.

3.1. Determination of the matrix elements

The determination of the matrix elements will be shown for the buck regulator.

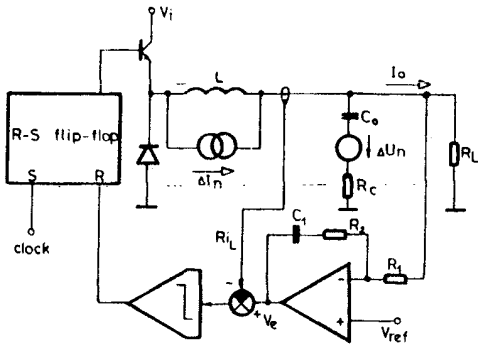

Fig.7 Constant-frequency current-mode controlled buck regulator with perturbations

There are two storage elements in the circuit: the filter inductor and the filter capacitor. Fig.7 shows the circuit with the generators which produce perturbation signal. Eq.(11) can be written in the form:

$$\begin{bmatrix} \Delta I_{n+1} \\ \Delta U_{n+1} \end{bmatrix} = \begin{bmatrix} a_{11} & a_{12} \\ a_{21} & a_{22} \end{bmatrix} \begin{bmatrix} \Delta I_n \\ \Delta U_n \end{bmatrix} \tag{15}$$

In order to calculate a_{11} and a_{21} let us assume: $\Delta U_n = 0$. The effect of the current perturbation on the waveforms of the circuit can be seen in Fig.8.

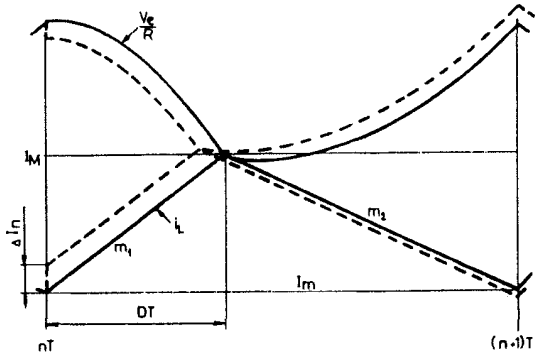

Fig.8 Waveforms in steady state and in perturbed state

Let the perturbation of the inductor current enter the system at the beginning of the nth period. This perturbation alters the current in the inductor and the voltage in the capacitor at the end of the same period. The following equations apply:

$$\Delta I_{n+1} = a_{11}\Delta I_n \quad \text{if} \quad \Delta U_n = 0 \tag{15a}$$

and

$$\Delta U_{n+1} = a_{21}\Delta I_n \quad \text{if} \quad \Delta U_n = 0 \tag{15b}$$

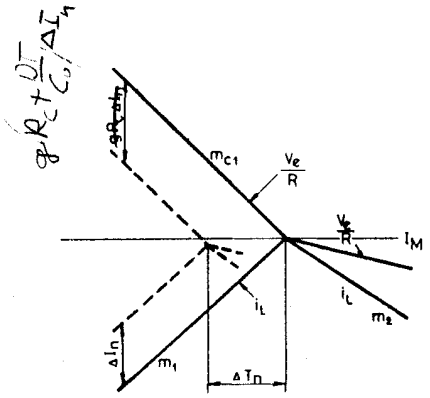

Fig.9 Waveforms in the vicinity of switch-over

ΔI_{n+1} can be determined by the help of Fig.9 which shows the current comparator waveform in the vicinity of the switch-over moment. From simple geometrical considerations:

$$\Delta T_n = \frac{\Delta I_n + g R_c \Delta I_n}{m_1 - m_{c1}} = g\left(R_c + \frac{DT}{C_o}\right)\Delta I_n \tag{16}$$

and

$$\Delta I_{n+1} = \Delta I_n + m_1(DT - \Delta T_n) + m_2[(1-D)T + \Delta T_n] \tag{17}$$

Eqs.(15a), (16) and (17) result in

$$a_{11} = \left.\frac{\Delta I_{n+1}}{\Delta I_n}\right|_{\Delta U_n = 0} = 1 - \frac{m_1 - m_2}{m_1 - m_{c1}}\left[1 + g\left(R_c + \frac{DT}{C_o}\right)\right] \tag{18}$$

The change in the voltage of the filter capacitor at the end of the period can be calculated as follows:

$$\Delta Q = \Delta I_n DT + \Delta I_{n+1}(1-D)T \tag{19}$$

The change in the capacitor voltage is

$$\Delta U_{n+1} = \frac{\Delta Q}{C_o} = a_{21}\Delta I_n \tag{20}$$

Combination of Eqs.(16), (17), (19) and (20) yields:

$$a_{21} = \left.\frac{\Delta U_{n+1}}{\Delta I_n}\right|_{\Delta U_n = 0} = \frac{T}{C_o}[D + (1-D)a_{11}] \tag{21}$$

The remaining matrix elements can be also easily calculated.

$$a_{12} = \left.\frac{\Delta I_{n+1}}{\Delta U_n}\right|_{\Delta I_n = 0} = g\,\frac{m_2 - m_1}{m_1 - m_{c1}} \tag{22}$$

and

$$a_{22} = 1 + g\frac{(m_2 - m_1)(1-D)T}{(m_1 - m_{c1})C_o} \tag{23}$$

In the above expressions m_1, m_2 and m_{c1} denote slopes of the inductor current and slope of the amplified and transformed ripple voltage. Their values are

$$m_1 = \frac{V_o(1-D)}{LD} \tag{24}$$

$$m_2 = -\frac{V_o}{L} \tag{25}$$

$$m_{c1} = -g\,\frac{V_o(1-D)}{LD}\left(R_c + \frac{DT}{2C_o}\right) \tag{26}$$

By the help of similar considerations the elements of matrix $\underline{\underline{A}}$ can be derived without difficulties for other topologies, too. Table 2 contains the results for the three basic converter circuits.

The slopes of the inductor current and of the feedback ripple are collected in Table 3.

3.2. Derivation of stability criteria

Eq.(14) gives possibility to derive the local stability criteria of the system. From the equation the eigenvalues of the perturbation matrix can be calculated by solving the resultant quadratic equation:

TABLE 2. PERTURBATION MATRICES

Buck $\underline{\underline{A}} =$

$$\begin{bmatrix} 1-\frac{m_1-m_2}{m_1-m_{c1}}\left[1+g\left(R_c+\frac{DT}{C_o}\right)\right] & g\frac{m_2-m_1}{m_1-m_{c1}} \\ \frac{T}{C_o}\left[D+(1-D)a_{11}\right] & 1+\frac{T(1-D)}{C_o}\,a_{12} \end{bmatrix}$$

Boost $\underline{\underline{A}} =$

$$\begin{bmatrix} \frac{m_2-m_{c1}}{m_1-m_{c1}} & g\frac{m_2-m_1}{m_1-m_{c1}} \\ \frac{T(1-D)}{C_o}a_{11} & 1+\frac{T(1-D)}{C_o}\,a_{12} \end{bmatrix}$$

Buck-boost $\underline{\underline{A}} =$

$$\begin{bmatrix} \frac{m_2-m_{c1}}{m_1-m_{c1}} & -g\frac{m_2-m_1}{m_1-m_{c1}} \\ -\frac{T(1-D)}{C_o}a_{11} & 1-\frac{T(1-D)}{C_o}\,a_{12} \end{bmatrix}$$

TABLE 3. EXPRESSIONS FOR m_1, m_2 AND m_{c1}

	m_1	m_2	m_{c1}
Buck	$\frac{V_o(1-D)}{LD}$	$-\frac{V_o}{L}$	$-g\frac{V_o(1-D)}{LD}\left(R_c+\frac{DT}{2C_o}\right)$
Boost	$\frac{V_o(1-D)}{L}$	$-\frac{V_oD}{L}$	$g\,\frac{I_o}{C_o}$
Buck-boost	$-\frac{V_o(1-D)}{LD}$	$\frac{V_o}{L}$	$-g\,\frac{I_o}{C_o}$

$$\lambda^2-\lambda(a_{11}+a_{22})+a_{11}a_{22}-a_{12}a_{21} = 0 \qquad (27)$$

There are two different ways to follow here. The simpler one is to assume first order subharmonic oscillation with infinitesimally small amplitude. This means an eigenvalue of -1. Then one can determine the corresponding transconductance g of the regulator from the equation:

$$1+a_{11}+a_{22}+a_{11}a_{22}-a_{12}a_{21} = 0 \qquad (28)$$

which is a quadratic formula for g with the starting conditions used.

The other, more general, way is to calculate the eigenvalues as functions of the loop transconductance and plot their absolut values versus g. If $|\lambda|=1$ we are at the verge of instability. This solution can take into account the theoretically possible complex roots and the case of $\lambda=1$.

According to our present experience the two methods give identical results for most practical circuit parameter combinations. Therefore the first one will be used further on. The details of the calculation are shown for the buck regulator.

Expressing the elements of the perturbation matrix by the help of the steady-state duty ratio and circuit parameters yields for the buck regulator:

$$a_{11} = -\frac{D+g\left[DR_c+\frac{D(1+D)T}{2C_o}\right]}{D'\left[1+g\left(R_c+\frac{DT}{2C_o}\right)\right]} \qquad (29)$$

$$a_{21} = -\frac{\frac{gDD'T^2}{2C_o^2}}{D'\left[1+g\left(R_c+\frac{DT}{2C_o}\right)\right]} \qquad (30)$$

$$a_{12} = -\frac{g}{D'\left[1+g\left(R_c+\frac{DT}{2C_o}\right)\right]} \qquad (31)$$

$$a_{22} = \frac{D'+g\left[D'R_c+\frac{D'T}{C_o}\left(\frac{D}{2}-1\right)\right]}{D'\left[1+g\left(R_c+\frac{DT}{2C_o}\right)\right]} \qquad (32)$$

Here $D' = 1-D$

Substituting the expressions of the matrix elements in Eq.(28) results in:

$$A\,g^2 + B\,g + C = 0 \qquad (33)$$

The coefficients of this equation are functions of the steady-state duty ratio D, the equivalent series resistance R_c and capacitance C_o of the output filter capacitor and the period time T. The exact expressions can be found in Table 4.

Eq.(33) can be easily solved by the help of a hand-held calculator. Some sample results are displayed in Section 5.

In a similar way the equations for the boost and buck-boost regulators can be also derived. As it is expected the transconductance at the boundary of instability is given by the roots of a quadratic equation which has the same form as Eq.(33) but has different expressions for the coefficients. These coefficients are also collected in Table 4.

Some interesting general conclusions can be drawn from the results shown in Table 4. The coefficients and so the stability conditions of the buck regulator do not depend on the inductance of the filter choke or on the load current. For the case of the boost and buck-boost regulator it can be established that the stability conditions do not depend on the equivalent series resistance of the output capacitor,

TABLE 4. COEFFICIENTS OF EQ.(33)

	A	B	C
Buck	$R_c^2(2-6D+4D^2)+\frac{R_cT}{C_o}(-1+4D-7D^2+4D^3)+$ $+\frac{T^2}{C_o^2}(-\frac{D}{2}+\frac{3D^2}{2}-2D^3+D^4)$	$R_c(4-12D+8D^2)+$ $+\frac{T}{C_o}(-1+4D-7D^2+4D^3)$	$2-6D+4D^2$
Boost	$\frac{4I_o^2L^2}{V_o^2C_o^2}+\frac{I_oLT}{V_oC_o^2}(1-D)$	$\frac{I_oL}{V_oC_o}(-6+8D)+$ $+\frac{T}{C_o}(-1+2D-D^2)$	$2-6D+4D^2$
Buck-boost	$\frac{4I_o^2L^2}{V_o^2C_o^2}D^2+\frac{I_oLT}{V_oC_o^2}(-D+D^2)$	$\frac{I_oL}{V_oC_o}(-6D+8D^2)+$ $+\frac{T}{C_o}(-1+2D-D^2)$	$2-6D+4D^2$

but depend on the inductance and the equivalent load resistance. In all three case the coefficient C vanishes at 50% duty ratio which means that here one of the roots of Eq.(33) will be zero. This indicates that instability occurs even at zero loop gain.

4. HYSTERETIC SUBHARMONIC INSTABILITY

Converters with constant-frequency or constant off-time controllers are inclined to a special form of subharmonic instability. The amplitude of oscillation in the state of this type of instability does not change with the loop gain, and the appearance of the instability is a hysteretic function of the gain. This means that the subharmonic oscillation starts at an upper gain level and ceases at a lower gain level.

The physical reason of the hysteretic subharmonic instability is very simple. If the loop gain is high enough to produce a fed-back ripple which does not allow the change of state of the current comparator, the system leaves out one period, i.e. it enters subharmonic oscillation. The current comparator cannot change state if the error signal with the superimposed ripple is below the inductor current at the next actual turn-on instant. As soon as the subharmonic operation takes place the output ripple suddenly increases in amplitude and prevents jumping back in the normal operating mode. Return to normal mode can occur only at a lower gain value. Of course, due to the hysteretic nature of this phenomenon, instability can appear even if the gain never exceeds the upper limit. External noise or transient, perhaps continuous subharmonic instability can push the system into this state. So from practical viewpoint the lower gain value is the border which the system must never exceed. There are cases where the upper limit is infinite. However, there is a lower finite value of the loop gain which must be respected because of the above discussed reason.

The boost and buck-boost regulators have a small step in the output voltage at the turn-on and turn-off instants. This step is due to the change in the current flowing in the equivalent series resistance of the output capacitor. If the incoming clock pulse (in the case of the constant-frequency controller) or the elapse of the pre-set off-time (constant off-time controller) can turn on momentarily the power switch the small jump in the output voltage alters the conditions of instability. Therefore two cases will be discussed. At the first one the condition of starting the subharmonic oscillation is as discussed previously. At the second one oscillation can start only if the feedback signal remains below the choke current even after the turn-on moment. The first one is called static and the second one is called dynamic turn-on. Fig.10 clarifies the distinction by the waveforms of the current comparator of a boost converter.

The upper gain limit can be calculated for both controllers (constant-frequency and constant off-time versions) from the equations which can be written according to Fig.10 (boost converter):

- dynamic turn-on $$g\frac{I_o}{C_o}T_{on} = m_1T_{on} \qquad (34)$$

- static turn-on $$g(\frac{I_o}{C_o}T_{on}+I_mR_c)=m_1T_{on} \qquad (35)$$

Similar equations can be produced for the buck-boost converter. The buck conver-

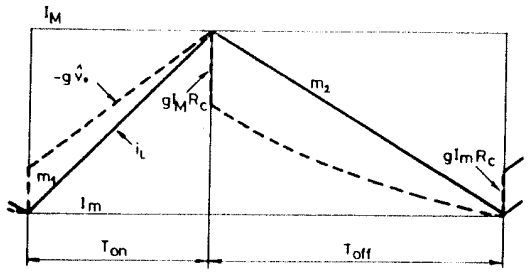

a) static turn-on

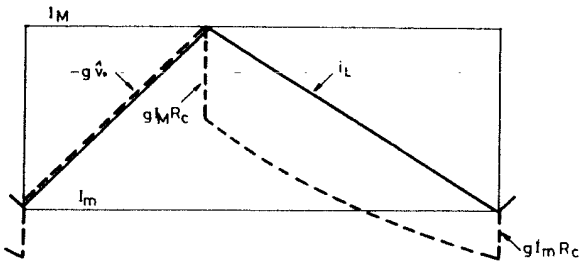

b) dynamic turn-on

Fig.10 Current comparator waveforms of a boost converter at the verge of hysteretic instability

ter is exception: here at the end of the period the fed-back output ripple is always above the inductor current and this means that the starting gain value is infinite.

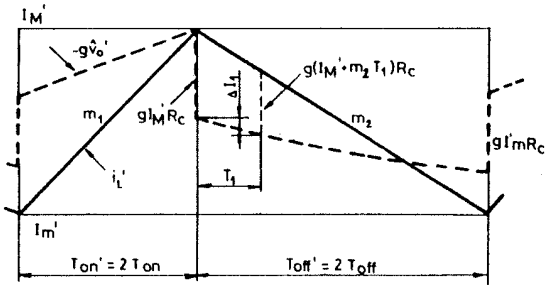

Fig.11 Waveforms of a boost converter in the state of hysteretic subharmonic oscillation

For the boost converter the lower gain limit can be calculated by the help of the waveforms in Fig.11. The waveforms are valid for the dynamic turn-on condition. The upper commas in the figure denote quantities in the state of subharmonic oscillation. The subharmonic oscillation ceases if the fed-back ripple becomes equal to the choke current during T_1 (after the turn-off moment). The value of T_1 is:

- for constant-frequency operation

$$T_1 = T\ (1-2D) \qquad (36)$$

- for constant off-time operation

$$T_1 = T_{off} \qquad (37)$$

The ceasing gain values can be determined from the following equations:

- dynamic turn-on

$$gI_M'R_c+\Delta I_1-g(I_M'+m_2T_1)R_c = -m_2T_1 \qquad (38)$$

- static turn-on

$$gI_M'R_c+\Delta I_1 = -m_2T_1 \qquad (39)$$

As in the case of the upper boundary the equations have the same form for the buck-boost converter. ΔI_1 can be calculated with the knowledge of the current flowing through the filter capacitor.

Lower gain limit exists for the buck regulator, too. It can be determined in the same way as in the two other cases.

Due to the limited space available the results are not submitted here. Those who are interested can request them from the authors. Partial results are presented in [6] and [13].

5. EXPERIMENTAL RESULTS

Two experimental circuits - a buck and a boost regulator - were built and measurements were made in order to verify the introduced theoretical results. Also two different types of controllers - constant-hysteresis and constant-frequency versions - were used. The measured data are shown in Figs.12-17 together with the appropriate calculated characteristics of the particular power circuit/controller combinations.

Fig.12 presents the actual operating frequency of a buck converter with constant hysteresis controller and at two different equivalent series resistances of the filter capacitor in function of the loop transconductance. Fig.13 and Fig.14 show the results of similar measurements for a boost converter with different R_C and C_O combinations. Here the correspondence between the calculated and measured values is not as good as in the previous case but still remarkable.

Fig.15 introduces the calculated transconductance-versus-gain function and the measured gains at the verge of instability for a buck regulator with constant-frequency controller. Here the correspondence between theory and experiments is surprisingly good, anyway it is much better than in a preceeding case which was based on describing function analysis [13]. The improvement is not so dramatic for the boost converter (Fig.16). Although the independence of the instability from the ESR, which is a new result since [13], is rather well demonstrated, the difference between prediction and measurements and the random deviations indicate the necessity of further refinements both in the theoretical model and in the experimental technique.

robably the inclusion of such second or- effects in the model as delay of the p er switch and/or the controller and mination of stray inductances at the test set-up would produce the required improvement. This might be the subject of a future study.

The hysteretic subharmonic oscillation was also demonstrated for the case of the static turn-on at a boost test circuit (Fig.17) with constant-frequency controller. Here the correspondence is also very good.

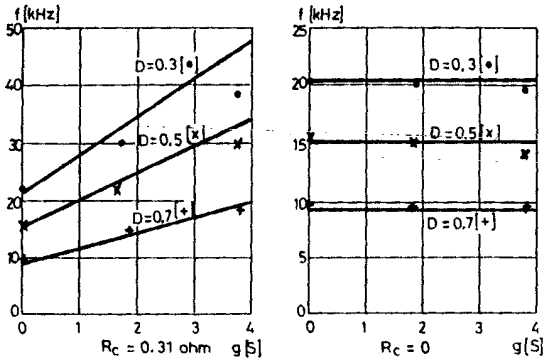

Fig.12 Calculated and measured frequency of a buck converter with constant--hysteresis controller (L=500μH; ΔI=0.66A; C_o=47μF)

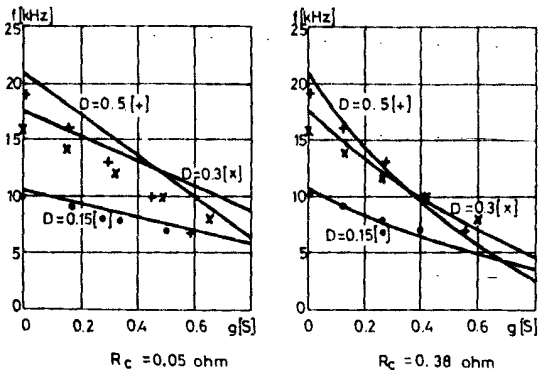

Fig.13 Calculated and measured frequency of a boost converter with constant-hysteresis controller (L=480μH; C_o=30μF; V_o=20V; I_o=0.5A; ΔI=0.5A)

6. CONCLUSIONS

Time domain analysis of waveforms of the current comparator in current-mode controlled switching voltage regulators seems to be a useful tool for the determination of stability criteria or for the prediction

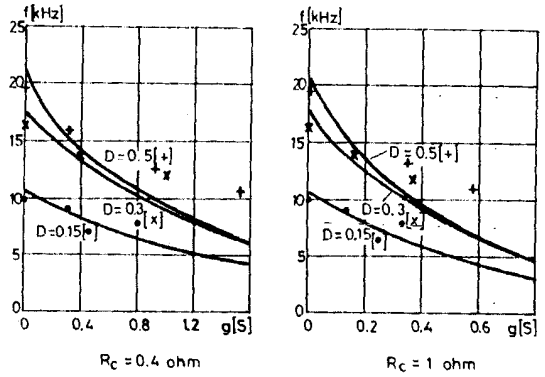

Fig.14 Calculated and measured frequency of a boost converter with constant--hysteresis controller (L=480μH; C_o=2200μF; V_o=20V; I_o=0.5A; ΔI=0.5A)

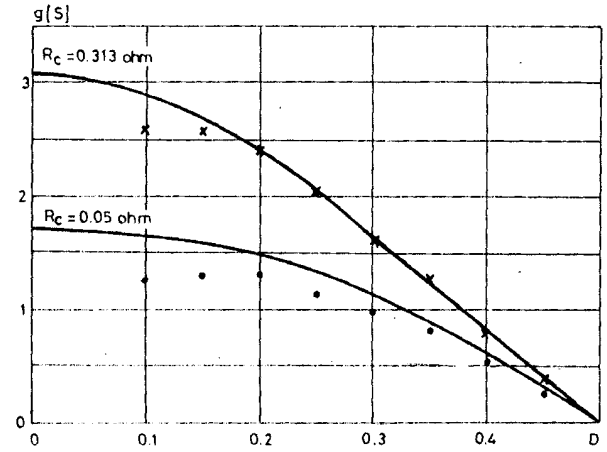

Fig.15 Calculated and measured transconductances of a buck regulator at the boundary of instability (C_o=47μF; T=60μsec)

of behavior at increasing ac gain values.

According to the experience of the authors three different closed-loop instability mechanisms are of outstanding importance at the above discussed class of power circuit/controller combinations. The hysteretically controlled converters display frequency shift but otherwise they are unconditionally stable. The constant--frequency controllers can result in continuously arising subharmonic oscillation which can be described by the help of perturbation analysis. Both the constant--frequency and constant off-time controllers are prone to hysteretically arising

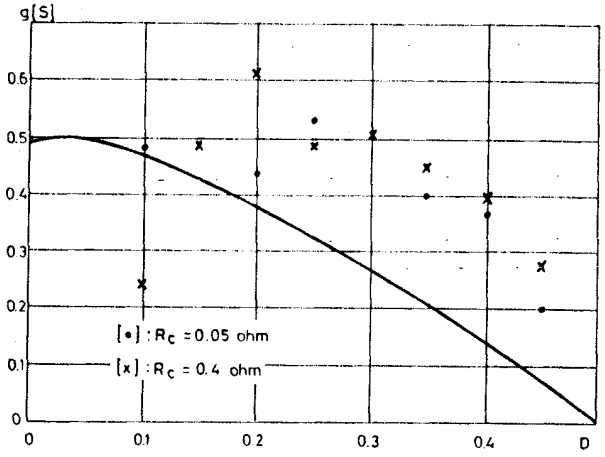

Fig.16 Calculated and measured transconductances of a boost regulator at the boundary of instability (V_O=20V; I_O=0.5A; L=480μH; T=60 μsec; C_O=30μF)

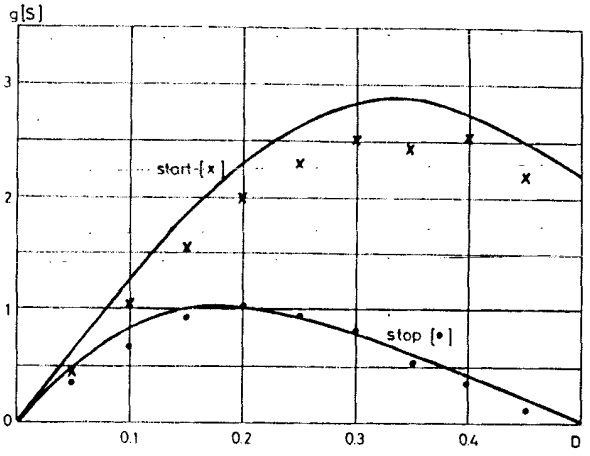

Fig.17 Calculated and measured transconductances for starting and ceasing hysteretic subharmonic oscillation at a boost regulator (V_O=20V; I_O=0.5A; L=480μH; T=60μsec; C_O=2200μF; R_C=0.4Ω)

subharmonic oscillation.

The presented stability criteria and expressions for frequency shifts produced predictions which were within measurement errors in most practical cases. Although the field is still open for further investigations in this area - especially to take into account some, until now neglected, second-order effects - the results give a rather complete characterization of the current-mode controlled voltage regulators from the viewpoint of loop-gain limitations.

REFERENCES

[1] T. Froeschle, "Two-State Modulation Techniques for Power Systems," Semi-Annual Report prepared by Bose Corp., for U.S. Army Electronics Command, 1967, Contract DA28-043-AMC-02281(E)

[2] A. Weinberg, D. O'Sullivan, "LC^3: Application to Voltage Regulation," Proc. of the Third ESTEC Spacecraft Power Conditioning Seminar (ESA Publication SP 126), 1977, pp.165-174.

[3] E. Pivit, J. Saxarra, "Upgrade Your Switchers Analytically," Electronic Design 10, May 10, 1978, pp.108-113.

[4] A. Capel, G. Ferrante, D. O'Sullivan, A. Weinberg, "Application of the Injected Current Model for the Dynamic Analysis of Switching Regulators with New Concept of LC^3 Modulator (Limit Cycle Conductance Controller)," PESC '78 Record (IEEE Publication 78CH1337-5 AES), pp.135-147.

[5] C. Deisch, "Simple Switching Control Method Changes Power Converter into a Current Source," PESC '78 Record (IEEE Publication 78CH1337-5 AES), pp.300-306.

[6] R. Redl, I. Novak, "Current-Mode Control of Switching Voltage Regulators, a New Method of Improving Regulation Parameters," (in Hungarian), Hiradastechnika, vol.29, no.11. 1978, pp.321-334.

[7] E. Pivit, J. Saxarra, "On Dual Control Pulse-Width Modulators for Stable Operation of Switched-mode Power Supplies," Wiss.Ber. AEG-TELEFUNKEN, vol.52 (1979), no.5, pp.243-249.

[8] Shi-Ping Hsu, A. Brown, L. Rensink, R. Middlebrook, "Modelling and Analysis of Switching DC-to-DC Converters in Constant-Frequency Current-Programmed Mode," PESC '79 Record (IEEE Publication 79CH1461-3 AES), pp.284-301.

[9] A. Capel, "Charge Controlled Conversion Principle in DC/DC Regulators Combines Dynamic Performance and High Output Power," PESC '79 Record (IEEE Publication 79CH1461-3 AES), pp.264-276.

[10] D. O'Sullivan, A. Weinberg, D. Levins, J. Schreuders, "SLIC^3: The Synchronised/Limit Cycle Conductance Controller," PESC '80 Record (IEEE Publication 80CH1529-7), pp.397-401.

[11] A. Capel, M. Clique, A. J. Fossard, "Current-Control Modulators - General Theory for Specific Designs," ESA Journal, 1980. vol.4. no.4. pp.397-416.

[12] R. Redl, N. O. Sokal, "Optimizing Dynamic Behavior with Input and Output Feed-Forward and Current-Mode Control," Proceedings of Powercon 7, 1980, San Diego, pp.H1-1 to H1-16.

[13] R. Redl, I. Novak, "Stability Analysis of Constant-Frequency Current--Mode Controlled Power Converters," Proceedings of the Second International Powerconversion Conference, 1980, Munich, pp.4.B.2-1 to 4.B.2-14.

[14] R. Redl, "Comparative Analysis of Overload Protection Methods for Switching-Mode Voltage Regulators," Proc. of the Third ESTEC Spacecraft Power Conditioning Seminar (ESA Publication SP 126), 1977, pp.155-164.